JOURNAL OF MATERIALS SCIENCE **36** (2001) 4687–4693

Investigations into the fracture mechanics of acetylsalicylic acid and lactose monohydrate

F. PODCZECK
Department of Pharmaceutics, The School of Pharmacy, University of London, 29/39 Brunswick Square, London WC1N 1AX, UK
E-mail: fridrun.podczeck@ams1.ulsop.ac.uk

The fracture mechanics of acetylsalicylic acid (ASS) and lactose monohydrate (LM) were studied using three-point beam bending experiments and compared with conventional tabletting performance. ASS was found to have an unusual behaviour in terms of its Young's modulus and tensile strength when determined with beams of different porosities. The Young's modulus as a function of beam porosity showed two exponential parts separated by a constant region and the tensile strength as a function of the porosity followed a non-exponential law. Tabletting experiments revealed that ASS undergoes different deformation mechanisms at the different compaction pressures associated with the porosity ranges covering the different regions. The different deformation mechanisms might have caused different crack and flaw patterns or different crack lengths, in particular at the beam surfaces, which are under maximum tensile stress during the tests. The unusual findings were, however, not reflected in experiments to determine the critical stress intensity factor as a function of beam porosity, because here crack propagation is controlled via a notch introduced into the beams. In contrast to ASS, LM behaved like the majority of materials i.e. Young's modulus, tensile strength and critical stress intensity factor were found to relate to the beam porosity exponentially.

Nomenclature

ASS	acetylsalicylic acid
A	notch depth
B	beam width
b	constant
D	beam thickness
d	distance between the mid point of one lower roll and the mid point of the beam (Equation 1); particle size (Equation 8)
E	Young's modulus
E_0	Young's modulus at zero porosity
G_{IC}	critical strain energy release rate
J_{IC}	fracture toughness
J_{IC}^{P}	plastic component of the fracture toughness
K_H	slope of the linear portion of the Heckel function
K_{IC}^{I}	critical stress intensity factor in mode I loading
K_{IC0}^{I}	critical stress intensity factor at zero porosity
K_P	yield pressure (Heckel function)
L	distance between the lower support rolls
LM	lactose monohydrate
P	breaking load
P_{lin}	load at the end of the linear portion of the stress–strain curve
p	porosity
R^2	determinant (non-linear regression analysis)
RMS	root mean square deviation (residual analysis)
Y^B	calibration factor
Y^D	calibration factor
Δ	beam deflection at the mid point of the beam
Γ	interfacial fracture energy
Γ_P	plastic component of the critical strain energy release rate
λ	stress singularity factor
ν	Poisson's ratio
σ_t	tensile strength
σ_{t0}	tensile strength at zero porosity
σ_Y	yield strength

1. Introduction

Tablets are still the most commonly administered dosage forms in Health care and medical treatment of patients. Their manufacture is cheap and the processing machines are highly optimised. Also in the future i.e. in the "century of gene therapy" tabletting is likely to remain one of the most important technologies due to the low costs and very good patient compliance. Drug substances to be compacted, however, will change in their physical properties. In the pharmaceutical industry the process of tablet making as such has been made to work, but little attention has been paid to the basic understanding of the physical processes involved. Only limited information is available on physico-mechanical properties of pharmaceutical powders, and which influence the latter have on the formation and properties of tablets. The majority of new tablet formulations are developed

by trial-and-error or by systematic variation of "preferred" excipients until a suitable formulation has been found. A choice of the quality and quantity of the excipients on the basis of physical data of the drug substances has rarely been done. Processes such as pharmaceutical tabletting could, however, be improved with a scientific foundation if the theory of fracture mechanics and its measurement techniques were considered.

There are some reports in the pharmaceutical literature, which provide fracture mechanics data of drug substances and excipients [1–8]. However, a comparative study [9] has shown that, if various sources are compared, these data are often very different in magnitude. One main reason for the variability appears to be inconsistencies in the techniques employed. Criteria with respect to beam dimensions were not clearly defined. Also, different beam porosities were achieved by changing the compaction pressure with a constant beam weight, which produces beams of different thickness. Yet these were used in extrapolations to zero porosity. With respect to the determination of the critical stress intensity factor, in some of the above references the crack length employed was not mentioned or not controlled, or the choice for a particular crack length used in the experiments was made arbitrarily. Also, extrapolations to zero porosity values often suffered from a lack of data close to zero porosity or at least below a porosity of 0.1. This affects not only the extrapolated values reported, but also the proof of the validity of the model equations employed in the extrapolations. Finally, the reports usually are restricted to yield strength, Young's modulus and critical stress intensity factor in mode I loading.

The aim of this paper was to study the fracture mechanics of two model substances—acetylsalicylic acid (ASS) and lactose monohydrate (LM)—and to compare the data derived with known tabletting properties. ASS is usually described as ductile material with large degree of plastic deformation [10, 11]. However, at higher tabletting forces extreme elastic deformability was also reported [12]. Large ASS crystals cannot be compacted into tablets, whereas fine powder particles provide mechanically appropriate tablets, when compressed at a low tabletting velocity. A change in the crystal density during compression at higher loads was suspected [13]. For LM, the findings are somewhat contradicting as both ductility [14] and brittleness [12, 15] during compression have been reported. LM crystals appear to be more than 6 times as hard as ASS crystals (indentation hardness 87 MPa [16] and 523 MPa [17] for ASS and LM, respectively).

2. Materials and methods

The following powders were used: Acetylsalicylic acid (ASS, Rütgers Organics GmbH, CF Aubing Pharmaceuticals, Mannheim, Germany, batch 98070230), lactose monohydrate (LM, Borculo Whey Products, Saltney, UK, batch 826704). The particle size was determined using light microscopy (Olympus BH-2, Tokyo, Japan) in connection with image analysis (Seescan Solitaire 512, Cambridge, UK). One thousand particles were inspected, and the mean Feret diameter was determined to be 8.8 ± 4.8 μm and 6.1 ± 3.9 μm for ASS and LM, respectively. The particle density was determined with an air pycnometer (Model 930, Beckman Instruments Inc., USA) and is 1540 ± 1 kg m^{-3} and 1400 ± 2 kg m^{-3} for LM and ASS, respectively (arithmetic mean and standard deviation of 5 replicates).

The powder specimens were manufactured on an Instron TT universal testing machine (Instron, High Wycombe, UK) at a compaction rate of 1 mm/min, and on a hydraulic press (Specac 15,000, Specac Ltd., Kent UK). The specimens were compacted to have a thickness of 5 mm after removal from the die. The compaction forces were recorded using a X–Y-recorder (Gould, model 6000, Bryan Southern Ltd., Surrey, UK). Different beam porosities were achieved by varying the specimen weight.

A specially manufactured split-die system was used, which can be dissembled completely, as long as the pressure exerted by the powder compact allows opening. The nominal dimensions of the die are length 45 mm and width 9 mm. With a thickness of 5 mm required to use the calibration functions reported by Brown and Srawley [18] the nominal volume of the beams is 2.025 cm^3. For the calibration experiments (determination of the notch depth for critical stress intensity factor measurements) 30 compacts with a porosity of 0.2 were produced. For all other experiments, 32 (LM) or 55 (ASS) compacts were manufactured, whereby the porosity of the specimens after unloading was between 0.2 and 0.02 (ASS), and between 0.2 and 0.07 (LM).

To determine Young's modulus and the tensile strength unnotched beams were used, and the values were calculated from the following equations (three-point beam bending):

$$E = \frac{P_{\text{lin}}}{\Delta} \frac{2d^3}{BD^3} \tag{1}$$

$$\sigma_{\text{t}} = \frac{3L}{2BD^2} P \tag{2}$$

where $E =$ Young's modulus, $P_{\text{lin}} =$ load at the end of the linear portion of the stress–strain curve, $P =$ breaking load, $\Delta =$ beam deflection at the mid point of the beam corresponding to P_{lin}, $d =$ distance between the mid point of one lower roll and the mid point of the beam, $B =$ beam width, $D =$ beam thickness, $\sigma_{\text{t}} =$ tensile strength and $L =$ distance between the lower support rolls.

To determine the mean yield strength, the tabletting pressure–porosity data were fitted to the Heckel function [19]. As the porosity of the beams was determined after removal of the specimens from the die, the yield strength σ_{Y} can be obtained from [20]:

$$\sigma_{\text{Y}} = \frac{1}{3K_{\text{H}}} = \frac{K_{\text{P}}}{3} \tag{3}$$

where $K_{\text{H}} =$ slope of the linear portion of the Heckel function, and $K_{\text{P}} =$ yield pressure derived from K_{H}.

For the determination of the critical stress intensity factor in mode I loading, K^{I}_{IC}, notches with an opening

angle of 90° were inserted into the beams using a miniature file. The notches were measured on both sides using the microscope attached to an image analyser (see above). The magnification was chosen, so that the standard imaging error of 1 pixel resulted in a measuring error of ±5.714 μm. Two possible calculation algorithms were compared:

1. The algorithm described by Brown and Srawley [18]:

$$K_{IC}^{I} = \frac{3}{2}\frac{LPa^{1/2}}{BD^2}Y^{B} \quad (4)$$

where Y^B is a calibration factor, and a = notch depth.

2. The algorithm described by Dunn *et al.* [21], which considers the geometry of the notch:

$$K_{IC}^{I} = \frac{3}{2}\frac{LP}{BD^2}D^{1-\lambda}Y^{D} \quad (5)$$

where Y^D is also a calibration factor, λ = stress singularity factor ($\lambda = 0.5445$ for a notch angle of 90°). The values for Y^B and Y^D are not identical. Details can be found in the original papers or in a summary by Podczeck [22].

The breaking load of the beams was obtained on a universal strength tester at a test speed of 1 mm/min (CT-5, Engineering Systems, Nottingham, UK) using a 5 kg load cell. A three-point bending rig with a lower span of 36 mm was used, and the beam deflection at its mid point was obtained from the chart recording. All measurements showed completely unstable crack propagation as defined by Adams [23] i.e. the stress–strain profiles were perfectly linear until catastrophic failure occurred.

All beams were stored for at least 2 weeks at room temperature and 40–45% relative humidity of the air. Twenty-four hours before the experiments the specimens were transferred into a desiccator filled with saturated solution of magnesium nitrate (BDH, Poole, UK) i.e. stored under controlled humidity of 53%. Afterwards the specimens were weighed (electronic recording balance, Sartorius, Göttingen, Germany) and measured (electronic callipers; length ± 0.01 mm; width and thickness ± 0.001 mm). The porosity of the specimens was calculated from these data and the density of the materials. The notches were inserted and measured as described above, and the breaking load was determined. All calculations were undertaken using SPSS 9.0 (SPSS Inc, Woking, UK). Non-linear relationships were always treated with non-linear regression to minimise errors when obtaining extrapolations to zero porosity.

3. Results and discussion

3.1. Powder compression and yield strength

After removal of the beams from the die they were measured immediately to confirm that they had the target thickness of 5.00 ± 0.01 mm. However, after two weeks of storage and calibration at 53% relative humidity, most of the beams had further expanded in all three dimensions. The final beam dimensions were $45.24 \pm 0.02 \times 9.04 \pm 0.01 \times 5.01 \pm 0.04$ mm^3 and $45.31 \pm 0.02 \times 9.05 \pm 0.01 \times 5.00 \pm 0.07$ mm^3 for ASS and LM, respectively. The thickness criteria ($4 \leq L/D \leq 8$) defined by Brown and Srawley [18] to be able to employ their calibration factor in Equation 4, however, was not violated by these changes, nor will the small differences in height be a reason for variability in the stress developing during beam bending.

The tabletting behaviour of the two materials was found to be very different. In order to produce beams below a porosity of 0.2, the hydraulic press had to be employed for LM. The minimum porosity that could be achieved with a maximum load of 15,000 kg available was 0.07. ASS is a much softer powder, and beams down to a porosity of 0.09 could be made at the Instron (maximum load capacity 2000 kg). Lower porosities were achieved using the hydraulic press. As the latter has no mechanisms to control the rate of loading, a series of beams were made to overlap the porosities achieved by the Instron. It is assumed that similar data in this overlapping range are sufficient to validate that the change of tablet press did not grossly influence the results found.

From the compaction forces recorded and the porosities of the beams after storage and calibration, Heckel plots were constructed. For either material five such plots, consisting of 32 (LM) or 55 (ASS) data points each were produced and the yield strength determined from the linear portions. Examples are provided in Fig. 1. For ASS, the Heckel plots were linear in the range of compaction pressures of 60–150 MPa, whereas for LM linearity did not occur below 100 MPa but remained above this pressure. Hence, under the experimental conditions used here, LM behaved ductile as reported by Duberg and Nyström [14]. The brittle behaviour found for ASS above 150 MPa has not been reported previously. The yield strength values obtained are 36.7 ± 1.7 MPa and 91.6 ± 9.4 MPa for ASS and LM, respectively. The yield strength found for ASS is close to literature values [10], but the value for LM

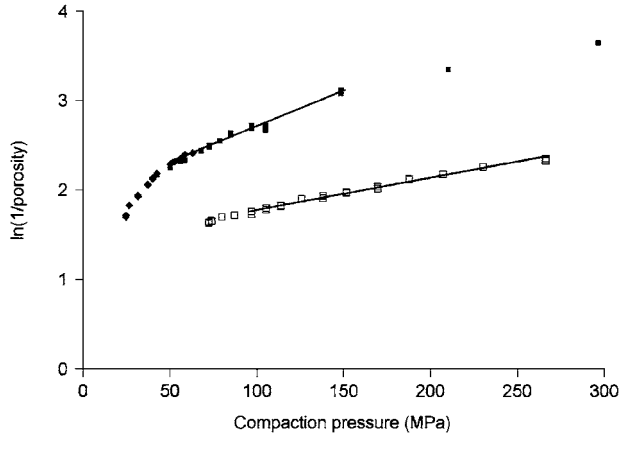

Figure 1 Heckel functions for acetylsalicylic acid (closed symbols) and lactose monohydrate (open symbols). The individual specimens were prepared using the hydraulic press (■) or the Instron (♦).

is comparatively small. Usually values of about 180 MPa are reported [24]. One possible reason could be the strain rate sensitivity of LM, but also the geometry and size of the specimens (larger beams instead of small round tablets) could have affected the results. York [25] found that a series of extrinsic factors can influence the yield strength values derived from Heckel functions, but in particular the size of the die was found to have a considerable influence. Hence, yield strength values derived from Heckel functions are not strictly material constants. The values reported here only apply for the experimental conditions used in this paper; a fact often overlooked in the pharmaceutical literature. Under the experimental conditions employed in this study the yield strength of LM is more than twice that of ASS. ASS is, therefore, the softer material. This ratio does not reflect, however, the six-fold difference between the crystal hardness values, but the latter are from different authors [16, 17] and using different indentation methods.

3.2. Young's modulus and tensile strength

The determination of the Young's modulus was made using unnotched specimens and the breaking load was used to calculate the tensile strength of the beams. All beams deformed fully elastic until catastrophic failure occurred i.e. the stress–strain diagrams were all linear.

The relationship between Young's modulus and beam porosity is illustrated in Fig. 2. For LM the data could be fitted to Spriggs' equation [26] ($R^2 = 0.976$, RMS = 2.30%). ASS showed a relationship not reported in the literature to date. Below a porosity of 0.09 there is an exponential change in Young's modulus as a function of beam porosity ($R^2 = 0.877$, RMS = 3.41%) as is above a porosity of 0.12. In the range between 0.09 and 0.12, however, the Young's modulus remains nearly constant. One reason for such behaviour could be a large amount of plastic deformation, but in such case the Young's modulus should not increase below a porosity of 0.09. A different explanation could be sought in the pore distribution of the beams. A rough estimate about the distribution and size of pores in solid specimen can be obtained from optical light microscopy [27] if a powerful light source is used. Inspection of the beams, however, confirmed a random pore distribution in all ASS beams independently of porosity. The onset of the upper exponential region (Fig. 2; porosity <0.09) coincides with the beginning of the linear region of the Heckel plots (Fig. 1) i.e. a compaction pressure of >60 MPa. The region below the linear portion of the Heckel function is regarded to be a reflection of densification due to fragmentation as any non-linear portion of such function. Hence, the plateau range (porosity values 0.09–0.12) for Young's modulus of ASS in Fig. 2 could be a result of an equilibrium of structural faults within and at the surface the beams, because fragmentation during compaction causes the formation of new surfaces at the same time as surfaces are welded together by bond formation. Crystal lattice changes such as twinning or crystal density changes [13] are less likely, because ASS has a monoclinic crystal lattice structure [28].

The extrapolated zero porosity Young's moduli for ASS (upper exponential region only) and LM were found to be 1.84 ± 0.03 GPa and 2.99 ± 0.06 GPa, respectively. In the literature, for ASS with a mean particle size of 32 μm a Young's modulus of 7.5 GPa was reported, and for LM of mean particle size of 20 μm a value of 24.1 GPa [29]. The differences in particle size between the tested powders and those used in the literature reports appear not large enough to account for the different findings. Bin Baie *et al*. [9] determined the Young's modulus for ASS to be 3.68 GPa, and for LM values between 6.44 and 6.66 were found. In either case, similar particle sizes to those used in this study were investigated. One possible reason is the different manufacture of the beams (control of storage time and storage conditions plus rate of compaction of 1 mm/min in this study), and different beam dimensions could also have contributed to the different observations.

The relationship between tensile strength of the beams and porosity is illustrated in Fig. 3 for both materials. Again, while LM provided a typical exponential relationship for pharmaceutical materials and ceramics, as described by Ryshkewitch [30] and Duckworth [31],

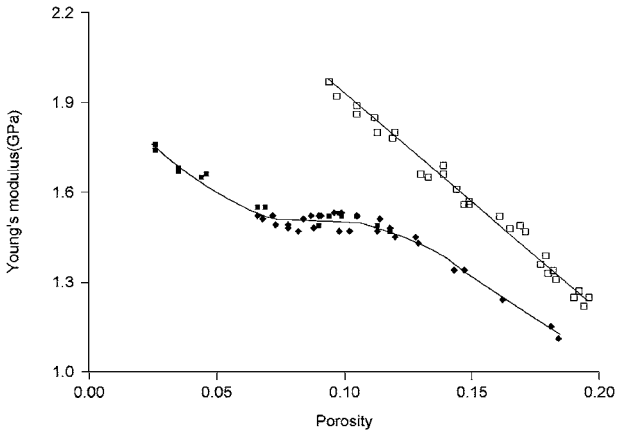

Figure 2 Young's modulus as a function of porosity for acetylsalicylic acid (closed symbols) and lactose monohydrate (open symbols). The individual specimens were prepared using the hydraulic press (■) or the Instron (♦).

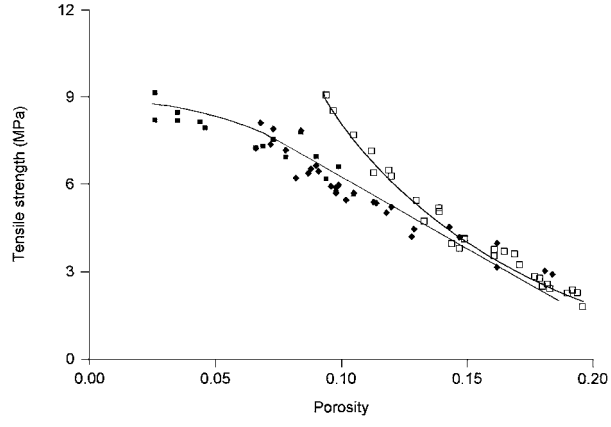

Figure 3 Tensile strength as a function of porosity for acetylsalicylic acid (closed symbols) and lactose monohydrate (open symbols). The individual specimens were prepared using the hydraulic press (■) or the Instron (♦).

ASS followed a relationship first reported by Dewey [32] for the Young's modulus as a function of porosity ($E = E_0(1 - \mathrm{bp})$). Tensile strength is only indirectly related to porosity via the Young's modulus of the specimens [33], and hence the application of Dewey's equation to describe the tensile strength σ_t as a function of beam porosity p ($\sigma_t = \sigma_{t0}(1-\mathrm{bp})$) appears justifiable. The occurrence of this tensile strength–porosity relationship for ASS indicates an over-proportional increase in beam elasticity at higher compaction pressures, as previously observed by Mielck and Stark [12] during conventional tabletting experiments. The zero porosity tensile strength for LM and ASS, obtained from the individual model functions, was calculated to be 33.0 ± 1.5 MPa ($R^2 = 0.985$, RMS = 6.92%) and 9.8 ± 0.2 MPa ($R^2 = 0.859$, RMS = 5.95%), respectively. LM specimens possess thus a considerably higher tensile strength than ASS specimens. Hence in composites (i.e. tabletting mixtures) this material should improve the mechanical properties of the compacts.

3.3. Critical stress intensity factor in mode I loading

The value of K_{IC}^{I} depends on the depth of the crack length introduced to control crack propagation. Initially, the value increases with an increase in notch depth. However, eventually, a limiting notch depth is reached, above which the K_{IC}^{I} becomes a constant, independent of the notch depth [18]. It is therefore necessary to determine the K_{IC}^{I} using beams with a notch depth above the limiting value. Nowhere in the pharmaceutical literature was this problem addressed to date. Often, the depth of the notches used was even not mentioned, or no exact measurements were performed. As a result, the values for K_{IC}^{I} vary grossly in the pharmaceutical literature. However, in the physical literature some estimation methods are provided, yet they require estimates of K_{IC}^{I}, yield strength and other physical properties of the materials. As these are unknown or experimental values are available only it appeared more sensible to follow the calibration procedure described by Brown and Srawley [18].

To determine the values of K_{IC}^{I} again the 3-point beam bending method was used. The values of K_{IC}^{I} were calculated both from equations and calibration terms provided by Brown and Srawley [18] and by Dunn *et al*. [21].

Initially the notch depth was calibrated using beams of a nominal porosity of 0.2. It is assumed that the cracks and flaws of beams with a lower porosity are smaller, hence requiring a smaller notch depth to control the fracture process. Thus, a notch depth determined on beams with a porosity of 0.2 will suffice for beams with lower porosity to produce values of K_{IC}^{I} independent of the notch depth. In Fig. 4 the relationships between K_{IC}^{I} and notch depth are illustrated using the values calculated according to Equation 5. For ASS the minimum notch depth was found to be 620 μm, and for LM a minimum notch depth of 400 μm appeared to be correct. Any value above these threshold limits should give an

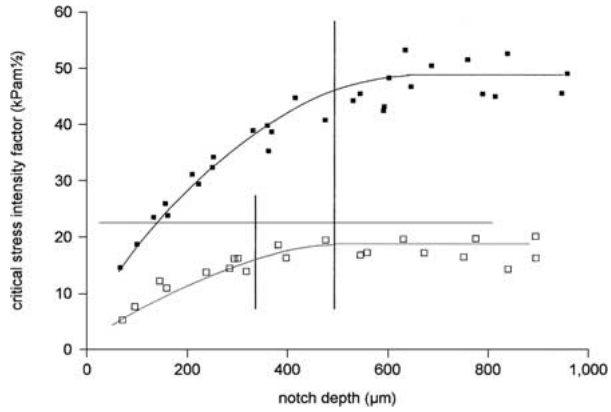

Figure 4 Critical stress intensity factor in mode I loading as a function of the notch depth for acetylsalicylic acid (closed symbols) and lactose monohydrate (open symbols). The individual specimens were prepared using the Instron and had a porosity of 0.2. Beyond the vertical lines the critical stress intensity factor is independent of notch length i.e. the minimum notch length is 620 μm and 400 μm for acetylsalicylic acid and lactose monohydrate, respectively.

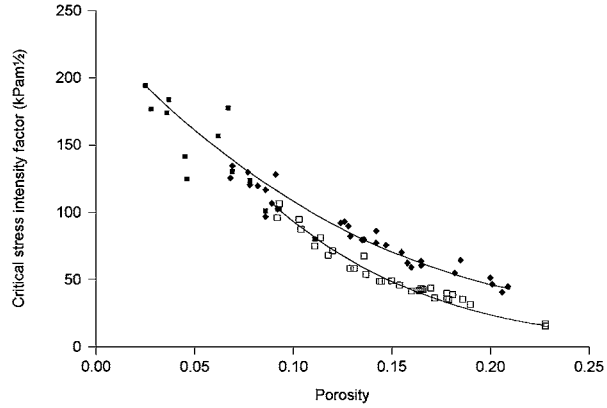

Figure 5 Critical stress intensity factor as a function of porosity for acetylsalicylic acid (closed symbols) and lactose monohydrate (open symbols). The individual specimens were prepared using the hydraulic press (■) or the Instron (♦).

appropriate value for K_{IC}^{I}. However, it appears better to keep the notch depth for all beams of one material reasonably similar.

In the next set of experiments it was aimed to get an estimate of the K_{IC}^{I} at zero-porosity. The average notch depths were 656 ± 62 μm and 865 ± 67 μm for LM and ASS, respectively. The two functions obtained are illustrated in Fig. 5 showing the results for the Dunn-approach.

The single values for K_{IC}^{I} of the beams are always higher using Equation 4 instead of Equation 5. Using Equation 4 (Brown and Srawley [18]) the zero porosity values are 366 ± 12 kPa $m^{1/2}$ ($R^2 = 0.925$, RMS = 5.18%) and 493 ± 32 kPa $m^{1/2}$ ($R^2 = 0.961$, RMS = 7.3%) for ASS and LM, respectively. Using Equation 5 (Dunn *et al*. [21]) for ASS 224 ± 8 kPa $m^{1/2}$ ($R^2 = 0.922$, RMS = 11.83%) and for LM 310 ± 18 kPa $m^{1/2}$ ($R^2 = 0.968$, RMS = 4.2%) were obtained. Both materials provide mono-exponential relationships (Fig. 5). The anomalies seen for ASS using unnotched beams to determine Young's modulus and tensile strength are not present here. The values for K_{IC0}^{I} for both materials are lower than those found in the literature [9].

From the values obtained for K^{I}_{IC0}, the critical strain rate energy release rate was calculated from:

$$G_{IC} = \frac{\left(K^{I}_{ICO}\right)}{E_O}(1 - \upsilon^2) \quad (6)$$

where the Poisson's ratio υ was assumed to be approximately 0.3. The G_{IC} values again vary in response to the equations used to determine K^{I}_{IC}. They were found to be 29.2 or 74.0 Nm^{-1} for LM and 24.8 or 66.2 Nm^{-1} for ASS, using the Dunn *et al*. [21] or Brown and Srawley [18] approach.

The fracture toughness, J_{IC}, has been shown to be numerically equal to G_{IC} values if these were determined from plain-strain experiments under predominant elastic conditions associated with sudden failure without prior crack extension [34]. The plastic component of this property can be found if the displacement at the mid point of the beams Δ is recorded during the bending experiments to obtain K^{I}_{IC} from:

$$J^{P}_{IC} = \frac{P\Delta/2}{BD - aD} \quad (7)$$

Here, values for J^{P}_{IC} of 8.7 ± 0.8 Nm^{-1} ($R^2 = 0.964$, RMS = 0.7%) and 5.9 ± 0.3 Nm^{-1} ($R^2 = 0.902$, RMS = 6.16%) were obtained for LM and ASS, respectively.

In order to validate the results obtained for K^{I}_{IC}, G_{IC} and J^{P}_{IC}, model calculations were performed. Kendall *et al*. [35] modelled G_{IC} of compacted powder specimens as:

$$G_{IC} = 56(1 - p)^4[\Gamma^5/E^2d^2]^{1/3} \quad (8)$$

where $\Gamma =$ interfacial fracture energy, and $d =$ particle size. Rearrangement of Equation 8 allowed the calculation of Γ to be 34.2 Jm^{-2} and 28.9 Jm^{-2} for LM and ASS, respectively. As G_{IC} is equal to 2Γ, the values for G_{IC} should approach 68.4 Nm^{-1} and 57.8 Nm^{-1}. If the Brown and Srawley [18] approach is considered, there is a good agreement between G_{IC} from experimental values for K^{I}_{IC0} and the values calculated above. The Dunn *et al*. [21] approach, however, results in values for G_{IC}, which are too small. Its general validity might hence be questionable. According to Adams [23], the critical strain energy release rate could be calculated from:

$$G_{IC} = 2\Gamma + \Gamma_p \quad (9)$$

where Γ_P is equivalent to the plastic component of G_{IC}, i.e. J^{P}_{IC}. Employing Equation 9, the values for $J_{IC}{}^{P}$ would be 11.2 Nm^{-1} and 16.8 Nm^{-1} for LM and ASS, respectively. These theoretical values are slightly higher than those obtained from experimental data, in particular for ASS.

3.4. Relationship between critical stress intensity factor and tensile strength

The general relationship between K^{I}_{IC} and σ_t is defined as [34]:

$$\sigma_t^2 = \frac{\left(K^{I}_{IC}\right)^2}{\pi a} \quad (10)$$

Employing Equation 10, the length of cracks propagated during beam bending can be estimated. Again, the results depend on whether Equation 4 or 5 is used to determine K^{I}_{IC}. When using Equation 4 [18], the crack length was calculated to be 70.9 μm and 447.6 μm for LM and ASS, respectively. Alternatively i.e. when using Equation 5 [21] values of 28.0 μm and 167.7 μm for LM and ASS, respectively, were obtained. The model calculations had indicated that Equation 4 arrives at more reasonable estimates of K^{I}_{IC} than Equation 5. Hence, cracks to be propagated in specimens made from ASS or LM appear to link pores along several particles, and crack propagation will more likely follow particle boundaries.

4. Conclusions

ASS was found to have an unusual behaviour in terms of its Young's modulus and tensile strength when determined from beams of different porosities. The Young's modulus as a function of beam porosity showed two exponential parts separated by a constant region and the tensile strength as a function of the porosity followed a non-exponential law. The unusual findings were, however, not reflected in experiments to determine the critical stress intensity factor as a function of beam porosity. To determine the latter, a notch was introduced large enough for the critical stress intensity factor to be independent of notch depth. As by this approach the surface and internal cracks and flaws of the original beams are excluded from propagation, the reason for the anomalies found must be related to the cracks and flaws present in the beams. From tabletting experiments employing the Heckel function it appeared as though ASS undergoes extensive particle fragmentation at lower compaction pressures, followed by a range of medium compaction pressures at which the material deforms elastically and/or plastically. At higher compaction pressures, the powder obviously starts to behave brittle again. The different deformation mechanisms might have caused different crack and flaw patterns or different crack lengths, in particular at the beam surfaces, which are under maximum tensile stress during the tests. In contrast to ASS, LM behaved like the majority of pharmaceutical powders i.e. Young's modulus, tensile strength and critical stress intensity factor were found to relate to the beam porosity exponentially.

Acknowledgements

I am very grateful to Professor Kevin Kendall for his comments and advice on the work, and his encouragement to write this paper. ASS and LM were gifts from Rütgers Organics GmbH, CT Aubing Pharmaceuticals

(Mannheim, Germany) and Borculo Whey Products (Saltney, UK), respectively. The work was partly financed by the Deutsche Forschungsgemeinschaft via a Heisenberg Fellowship.

References

1. A. B. MASHADI and J. M. NEWTON, *J. Pharm. Pharmacol.* **39** (1987) 961.
2. *Idem., ibid.* **39** (1987) 676P.
3. R. J. ROBERTS and R. C. ROWE, *Int. J. Pharm.* **52** (1989) 213.
4. F. BASSAM, P. YORK, R. C. ROWE and R. J. ROBERTS, *ibid.* **64** (1990) 55.
5. P. YORK, F. BASSAM, R. C. ROWE and R. J. ROBERTS, *ibid.* **66** (1990) 143.
6. F. PODCZECK and J. M. NEWTON, *Pharmazie* **47** (1992) 462.
7. J. M. NEWTON, A. B. MASHADI and F. PODCZECK, *Eur. J. Pharm. Biopharm.* **39** (1993) 153.
8. R. J. ROBERTS, R. C. ROWE and P. YORK, *Int. J. Pharm.* **91** (1993) 173.
9. S. BIN BAIE, J. M. NEWTON and F. PODCZECK, *Eur. J. Pharm. Biopharm.* **43** (1996) 138.
10. P. HUMBET-DROZ, R. GURNY, D. MORDIER and E. DOELKER, *Int. J. Pharm. Technol. Prod. Mfr.* **4** (1983) 29.
11. W. JETZER, M. DÜGGELIN, R. GUGGENHEIM and H. LEUENBERGER, *Acta Pharm. Technol.* **30** (1984) 126.
12. J. B. MIELCK and G. STARK, *Eur. J. Pharm. Biopharm.* **41** (1995) 206.
13. S. PEDERSEN and H. G. KRISTENSEN, *S. T. P. Pharma Sci.* **4** (1994) 201.
14. M. DUBERG and C. NYSTRÖM, *Acta Pharm. Suec.* **19** (1982) 421.
15. E. T. COLE, J. E. REES and J. A. HERSEY, *Pharm. Acta Helv.* **50** (1975) 28.
16. K. RIDGWAY, E. SHOTTON and J. GLASBY, *J. Pharm. Pharmacol.* **21** (Suppl.) 19S.
17. J.-I. ICHIKAWA, K. IMAGAWA and N. KANENIWA, *Chem. Pharm. Bull.* **36** (1988) 2699.
18. W. F. BROWN and J. E. SRAWLEY, *ASTM Special Technical Publication* **410** (1967).
19. R. W. HECKEL, *Trans. Metal. Soc. AIME* **221** (1961) 671.
20. *Idem., ibid.* **221** (1961) 1001.
21. M. L. DUNN, W. SUWITO and S. CUNNINGHAM, *Int. J. Solids Structures* **29** (1997) 3873.
22. F. PODCZECK, in "Particle–particle Interactions in Pharmaceutical Powder Handling" (Imperial College Press, London, 1998) p. 169.
23. M. J. ADAMS, *J. Powder Bulk Solids Technol.* **9** (1985) 4, 15.
24. R. C. ROWE and R. J. ROBERTS, in "Pharmaceutical Powder Compaction Technology," edited by G. Alderborn and C. Nyström (Marcel Dekker, New York, 1995) p. 283.
25. P. YORK, *J. Pharm. Pharmacol.* **31** (1979) 244.
26. R. M. SPRIGGS, *J. Amer. Ceram. Soc.* **44** (1961) 628.
27. U. MÜCKE, T. RABE and J. GOEBBELS, *Prakt. Metallogr.* **35** (1998) 665.
28. J. MAASZ and C. BEYER, *Pharm. Ind.* **49** (1987) 386.
29. R. J. ROBERTS, R. C. ROWE and P. YORK, *Powder Technol.* **65** (1991) 139.
30. E. RYSHKEWITCH, *J. Amer. Ceram. Soc.* **36** (1953) 65.
31. W. DUCKWORTH, *ibid.* **36** (1953) 69.
32. J. M. DEWEY, *J. Appl. Phys.* **18** (1947) 578.
33. R. W. RICE, *Mat. Sci. Engnr.* **A112** (1989) 215.
34. R. W. HERTZBERG, in "Deformation and Fracture Mechanics of Engineering Materials," 4th edn. (John Wiley & Sons, New York, 1996) pp. 337–362.
35. K. KENDALL, N. McN. ALFORD and J. D. BIRCHALL, *Spec. Ceram.* **8** (1986) 255.

Received 22 August 2000
and accepted 11 May 2001